

POST IRRADIATION EXAMINATION OF HIGH BURNUP PHWR FUELS

R.S. SHRIWASTAW, PRERNA MISHRA, PRITI K. SHAH, J.S. DUBEY,
V.P. JATHAR, H.N. SINGH, B.N. RATH, K.M. PANDIT, ANIL BHANDEKAR,
ASHWINI KUMAR, J.L. SINGH, G.K. MALLIK, SUNIL KUMAR AND ARUN KUMAR

*Post Irradiation Examination Division,
Bhabha Atomic Research Centre, Trombay, Mumbai, India*

ABSTRACT

Post Irradiation Examination (PIE) was carried out on 220 MWe pressurised heavy water reactor (PHWR) fuel bundles irradiated to a burnup of 10000 MWd/tU and 22000 MWd/tU to assess the performance of the fuel pins. Various non-destructive and destructive techniques used for the examination included visual examination, leak testing, profilometry, gamma scanning, ultrasonic testing, fission gas analysis, metallography of fuel and cladding, β - γ autoradiography of fuel sections and ring tension test (RTT) of the cladding. During PIE, no fuel failure was observed in any of the fuel pins of the two bundles. Circumferential ridges on the cladding, higher fission gas pressure and restructuring in fuel with formation of grain growth region was observed in outer pins of the high burnup fuel bundle. The RTT results indicated irradiation hardening and reduction in clad ductility at 25°C whereas significant increase in clad ductility was noticed at 300°C.

1. Introduction

Indian PHWRs use natural uranium as fuel in the form of UO₂ pellets. The average discharge burnup of PHWR fuel bundles is around 7000 MWd/tU and maximum burnups are around 15000 MWd/tU. These PHWRs have the experience of irradiation of bundles up to burnups of around 15000 MWd/tU on which PIE investigations have been carried out. The detailed examinations carried out earlier on these bundles have been reported elsewhere [1-4]. In order to improve the fuel economy of Indian PHWRs, it has been proposed to extend the average discharge burnup of fuel bundles. Few fuel bundles were irradiated to extended burnups in selected channels of Kakrapar Atomic Power Station (KAPS). Monitoring systems in the reactor during irradiation indicated successful performance of the fuel bundles [5]. In order to know the overall performance of the fuel pins after irradiation, two fuel bundles irradiated to a burnup of 10000 MWd/tU and 22000 MWd/tU were brought to the hot cell facility for PIE. The present paper describes the details of the examination carried out on these fuel bundles and the results obtained.

2. Fabrication details

A fuel bundle for a 220 Mwe PHWR consists of 19 fuel pins arranged in a circular geometry with 12 and 6 fuel pins in the outer ring and intermediate ring, respectively and a central fuel pin as shown in Fig. 1. The fuel pins contain UO₂ fuel pellets with nominal dimensions of 17 mm length and 14 mm diameter encapsulated in Zircaloy-4 cladding, which is hermetically sealed at both ends using end plugs. The cladding tube with outside diameter of 15.2 mm and 0.4 mm nominal wall thickness is joined to the end plugs by resistance welding. Helium is used as the filler gas in all the fuel pins. Appendages like bearing pads and spacer pads are spot welded on the fuel pins. The fuel pins are assembled into a fuel bundle by spot welding the end plugs to endplates. The overall length of the fuel bundle is 495 mm [6].

3. Irradiation History

Two fuel bundles irradiated to a burnup of about 10000 MWd/tU and 22000 MWd/tU (hence forth shall be written as bundle-1 and bundle-2, respectively) were received in the hot cell facility for PIE. Irradiation details of the two bundles irradiated in KAPS are given in Table-1[7].

Bundle No.	Bundle-1	Bundle-2
Burnup (MWd/tU)	10000	22000
Residence time (FPD)	255	800
Peak Power (kW)	340	450
Linear heat rating (kW/m)	40	54
Year of discharge from reactor	2009	2003

Table-1 Irradiation details of the fuel bundles

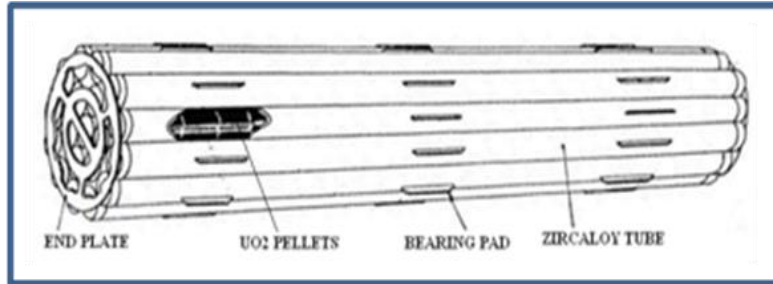


Fig.1 Nineteen pin fuel bundle for 220 MWe PHWR

4. Post Irradiation examination

After preliminary visual examination of the fuel bundles for their overall integrity, the fuel bundles were dismantled inside the hot cell to separate the fuel pins. The end plugs to endplates spot welds were cut by using power hacksaw. The end of a fuel bundle with and without the end plate is shown in Fig. 2. After bundle dismantling, the fuel pins were subjected to various non-destructive and destructive techniques for detailed post irradiation examination.

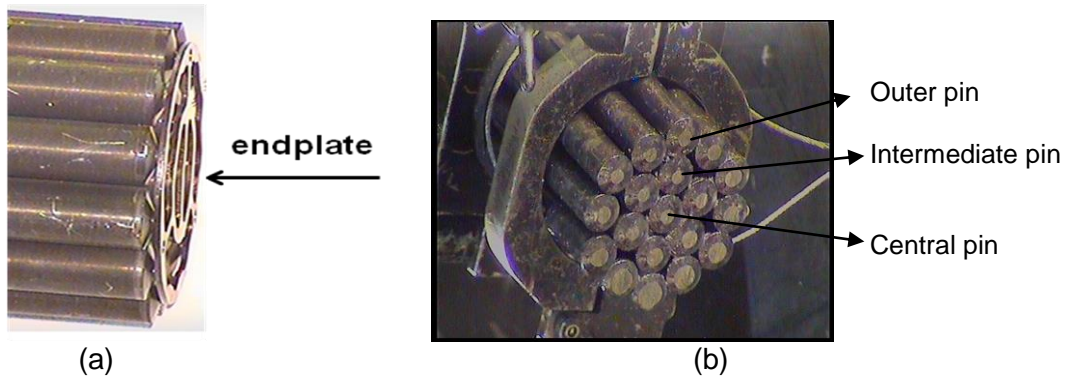


Fig.2: End of the fuel bundle (a) with endplate and (b) without endplate

4.1 Visual examination

All the fuel pins were cleaned and subjected to visual examination using a wall mounted camera to check the condition of all the welded appendages and also for the presence of surface defects like cracks, corrosion, discoloration, fretting, ridging, etc. For visual examination, each pin was placed horizontally on two rollers fitted on the table top in the hot cell in such a way that the pin faces the overhead camera directly. By rotating the pin on the rollers with the help of Master Slave Manipulators (MSMs), the entire surface of the fuel pin was examined. The fuel pin surface appeared dull dark in colour as compared to the metallic lustre of the unirradiated fuel pins. All the appendages of the fuel pins were found intact and the end cap welds of the fuel pins were found to be visually intact. In case of bundle-2, circumferential parallel lines were observed on all the outer fuel pins as shown in Fig. 3. The distance between these lines were measured using a scale and was found to be 17 mm, which corresponds to the pellet length.

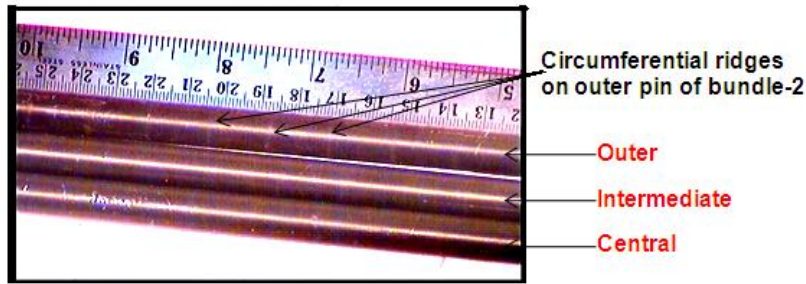


Fig.3: Circumferential ridges on the outer fuel pin of bundle-2

4.2 Leak testing

After visual examination, leak testing of individual fuel pins was carried out using liquid nitrogen-alcohol leak test method. The fuel pins were immersed in liquid nitrogen for 10 minutes. The pin was then taken out of liquid nitrogen and placed in alcohol bath at room temperature. The pin placed in the alcohol bath was continuously monitored by the camera to record the bubbles coming out of the fuel pin, in case of a leak. However, no leak was detected in any of the fuel pins of the two bundles.

4.3 Profilometry

Axial diameter profile of the fuel pins was obtained by using a laser profilometer. A laser micrometer is placed on a motorized linear motion stage. The fuel pins were placed in the pin holding grips and the laser micrometer was moved from one end to other end and the pin outer diameter data was recorded. Negligible change in diameter was observed along the length of the fuel pins of bundle-1. Bundle-2 showed an increase in diameter in its outer fuel pins. This increase was measured to be around 80-100 μm as compared to that of as-fabricated fuel pins. Also, a prominent increase in the fuel pin diameter at regular axial locations was noticed. These axial locations correspond to the circumferential lines observed during visual examination and increase in diameter, at these locations, indicate ridging in the fuel pin. The height of ridges ranged from 30-50 μm . Figs. 4 (a) and (b) show the diametral profile of the outer fuel pin of bundle-1 and bundle-2, respectively.

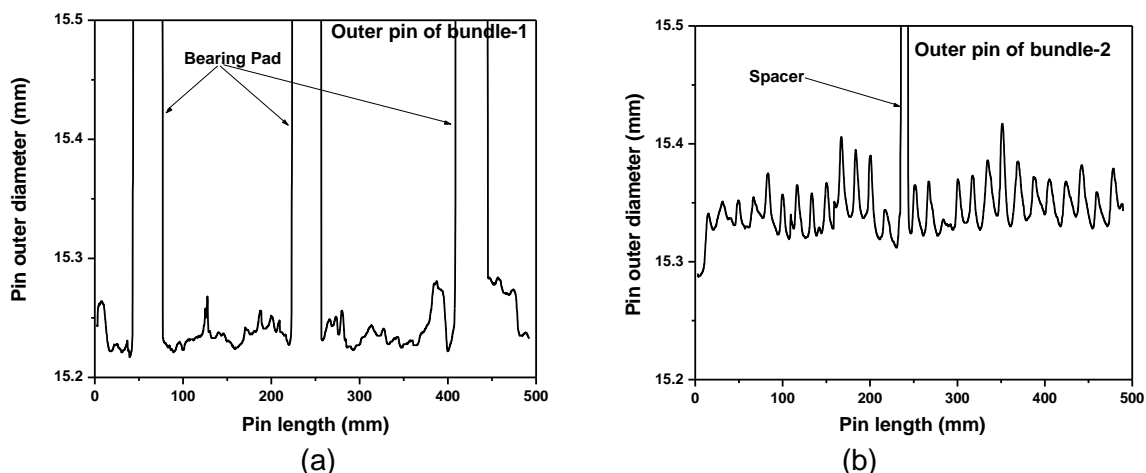


Fig. 4 Typical diametral profile of an outer fuel pin of (a) bundle-1 and (b) bundle-2

4.4 Gamma scanning

Gamma scanning was used to generate information on axial burn up distribution in the fuel pins. The measurement was based on a high-purity germanium detector (HPGe) together with mechanical arrangement for fuel pin movement across the detector with a speed of 0.07 mm/sec through a narrow collimator. The liquid nitrogen cooled HPGe detector provides energy resolution of 1.8 keV FWHM at energy 662 keV. Five numbers of fuel pins, two from outer ring, two from intermediate ring and the central pin from each the fuel bundles

were taken for the measurement. The gamma energy spectrum of the fuel pins of both the bundles showed distinct peaks of Cs^{137} (662 keV) and Cs^{134} (604 and 796 keV). A typical gamma energy spectrum of the outer fuel pin of bundle-1 is shown in Fig. 5 (a). Gamma scanning of the fuel pins was carried out by measuring the relative distribution of fission product, Cs^{137} along the length of the fuel pins. Gamma scan of the fuel pins of both the bundles showed uniform burn up distribution along the length of the fuel pin. Fig. 5 (b) shows the gamma scan of one of the outer fuel pins of bundle-2.

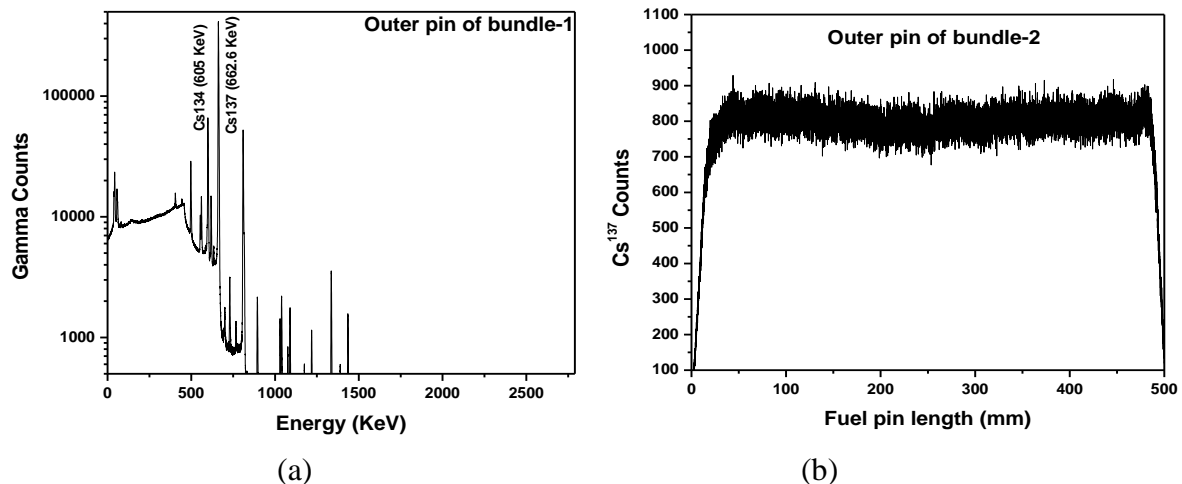


Fig.5 (a) A typical gamma energy spectrum of the outer fuel pin of bundle-1 and (b) Gamma scan of the outer fuel pin of bundle-2

4.5 Ultrasonic testing

Immersion Ultrasonic testing (UT) was carried out to detect the irradiation induced incipient flaws in the clad using probes of 15 MHz frequency and 20 mm spot focal length. For testing, the fuel pin was horizontally mounted on the scanning stage inside the cell. The stage was fitted with two motors; one for rotating the fuel pin and other for the horizontal movement of the UT probes. Two probes were used; one for circumferential scan and the other for axial scan. However, no defect was detected during testing of the fuel pins.

4.6 Fission gas analysis

The fuel pins were punctured in a specially designed and fabricated setup consisting of a puncture chamber which is connected to the vacuum pump, gas collection vessel and measuring manifold. The quantitative estimation of the gases was carried out by applying the standard gas laws after measuring the gas pressure using capacitance diaphragm gauge. Chemical composition of the gases was determined using a dual column gas chromatograph, with Argon as the carrier gas. Thermal conductivity detector was used for the detection of the individual gases. A quadrupole mass spectrometer was used for measuring the isotopic ratios of Xe and Kr. Other parameters such as system volume, system pressure, void volume of the fuel pin and the pressure / volume of the released gases in free volume of fuel pin were estimated by using the calibration flask with the system and by applying standard gas laws. The released fission gas (FG) pressure was found to be higher in outer pins as compared to the intermediate pins and the central fuel pin of bundle-2. The results of fission gas release measurement in the fuel pins of the two fuel bundles are given in Table-2.

Details	Fuel pins from Bundle-1			Bundle-2		
	Outer	Inter-mediate	Central	Outer	Inter-mediate	Central
Void volume (cc)	2.50-3.86	2.5	3.51	3.67-3.95	2.10	1.09
% Release as per Estimation	0.05-0.059	0.037	0.036	22.28-22.86	3.89	0.21

Table-2 Details of the released fission gas analysis for bundle-1 & bundle-2

4.7 Metallographic examination:

The fuel samples were cut from selected locations of the fuel pins (outer, intermediate and central) of both the bundles and prepared metallographically to get a polished sample. The samples were subjected to microscopic examination under a remotised-shielded metallograph. Images were grabbed and stored in the computer and image analysis was carried out to measure the grain size in the fuel, oxide layer thickness on the clad, etc.

Photomicrographs of fuel sections from the fuel pins of bundle-1 showed radial cracks and the intergranular porosity region was absent. Fig. 6 (a) shows a photomicrograph of the fuel section from the outer pin of bundle-1. Examination of the fuel section after etching revealed a marginal increase in the grain size at the central region of the fuel section taken from the outer and intermediate fuel pin. Grain size at the center of the fuel section taken from the outer, intermediate and central fuel pins was 15 μm , 14 μm and 11 μm , respectively. Grain size at the periphery of the fuel sections was in the range of 9-11 μm .

Fig. 6 (b) & (c) show the photomicrograph and β - γ autoradiograph respectively of the fuel section from the outer fuel pin of bundle-2. Severe cracking in the form of radial and circumferential cracks was observed in the fuel. The fuel section revealed intergranular porosity region with a fuel fractional radius of 0.67 and 0.32 in the outer and intermediate fuel pins, respectively. The intergranular porosity region was not observed in the fuel sections of the central fuel pin. The β - γ autoradiograph of the fuel section from outer fuel pin, shown in the Fig. 6 (c), shows a bright central region, which indicates the fission product (Cesium) depleted region. Bright region is observed to be maximum in the outer pin, lesser in the intermediate pin and least in the central pin. Average grain size revealed at the periphery and centre of the fuel section of the outer fuel pin of bundle-2 was 11 μm and 34 μm respectively.

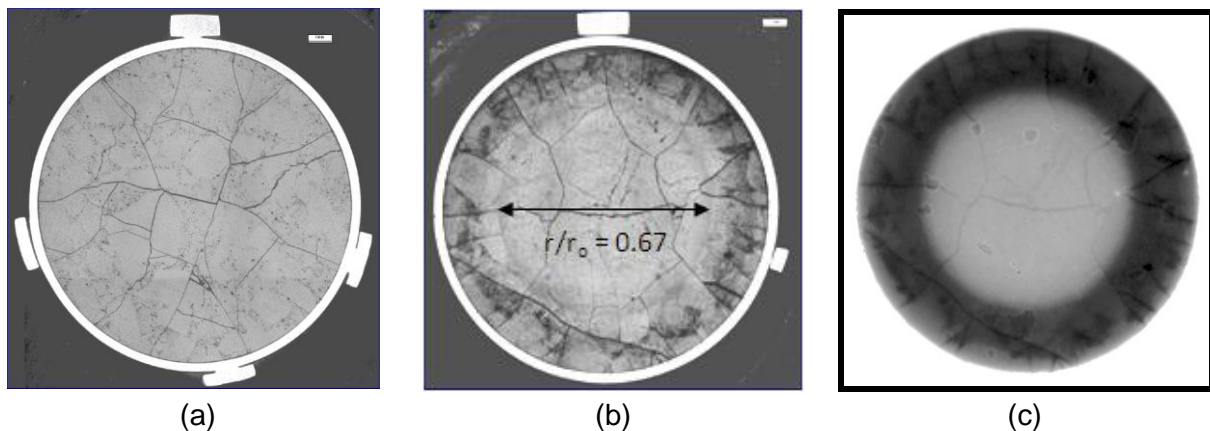


Fig. 6 Photomicrographs of the fuel section from the outer fuel pin of (a) bundle-1 and (b) bundle-2 and (c) β - γ autoradiograph of the fuel section from the outer fuel pin of bundle-2

4.8 Ring tension test (RTT)

Transverse tensile properties of fuel claddings were estimated by carrying out RTT on 3.5 mm wide rings prepared from the outer fuel pins of two bundles. The fuel pins were sliced in a slow speed cut-off machine using diamond impregnated wafering wheel and the slices were defueled to obtain the clad rings. After cleaning them in ultrasonic cleaner, the ring width was measured using digital vernier callipers. The rings were tested using two split semi circular mandrels attached to a set of grips as shown in Fig. 7. The RTT was carried out in a screw driven universal testing machine at a crosshead speed of 0.25 mm/min at two temperatures, 25°C and 300°C. Minimum three ring specimens from each of the two outer fuel pins of two bundles were tested at two test temperatures. The effective gage length was taken as 5.2 mm in this work and all the elongation values reported here are based on this gage length. The technique to determine the gage length of a ring specimen was standardised earlier and reported elsewhere [8].

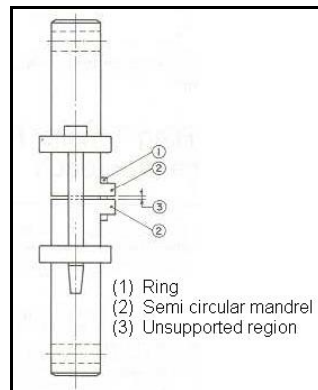


Fig. 7 Schematic of ring tension test grip

4.8.1 Transverse tensile behaviour of fuel claddings

The stress-strain curves obtained at temperatures 25°C and 300°C are shown in Fig.8 (a) and (b) respectively. The transverse tensile properties are given in Table-3. The total elongation (TE) obtained from as-fabricated clad was in the range of 28 - 30% at 25°C and 34 - 36% at 300°C. Comparing the stress-strain curves at two temperatures, it can be seen that the material hardening and loss of TE has occurred due to high energy neutron irradiation. At 25°C, the TE in the irradiated claddings has decreased to around 6 -10% and 5 - 7% for bundle-1 and bundle-2 respectively. The decrease in TE was observed more in the non-uniform part of the strain, though the uniform elongation (UE) had also decreased.

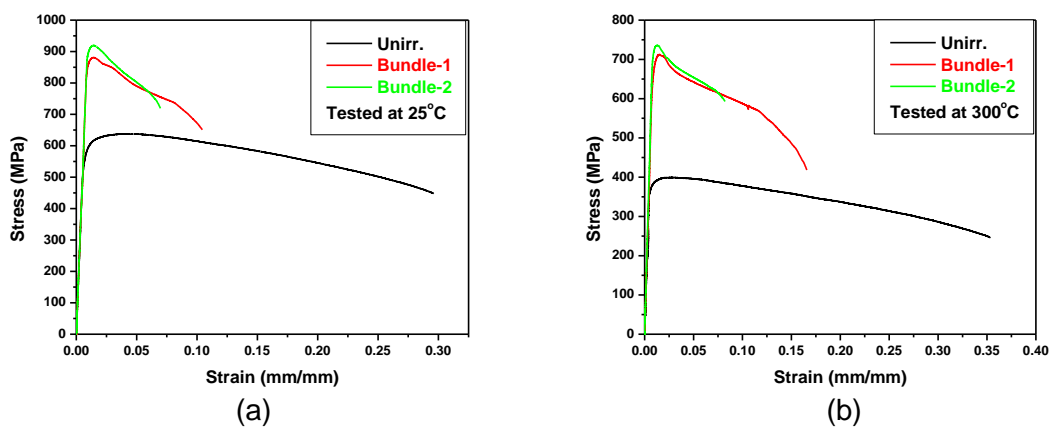


Fig. 8 Stress-strain curves at (a) 25°C (b) 300°C

At higher test temperature of 300°C the TE for both the bundles had increased significantly (Table-3). Though the higher flow stress due to irradiation hardening is evident the

specimens tested at this temperature, resulted in large variation in TE. Fig. 9 shows the variations observed in stress-strain curves obtained from three specimens tested at 300°C.

Materials	Test temp. (°C)	YS (MPa)	UTS (MPa)	UE (%)	TE (%)
As fabricated	RT	570-620	638-682	3.7-4.4	28-30
	300	372-373	400-404	2.6-2.8	34-36
Bundle-1	RT	797 - 955	840 - 1011	1.4 - 1.8	6 - 10
	300	677 - 691	686 - 692	1 - 1.5	12 - 24
Bundle-2	RT	853 - 911	890 - 928	1.4 - 1.5	5 - 7
	300	625 - 731	636 - 769	1.1 - 1.4	8 - 22

Table-3 Transverse tensile properties of the clad tubes

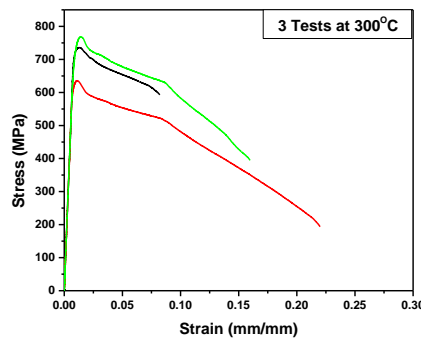


Fig. 9 Stress-strain curves obtained from three tests at 300°C for bundle-2

Fig. 10 compares the deformation behaviour of different claddings after testing. The as fabricated clad showed fully ductile rupture with prominent neck formation and thickness contraction at 25°C (Fig. 10 (a)) and the Irradiated clads resulted in shear band fracture at 45 degree to the loading axis, with little amount of deformation (Fig. 10 (b) and (d)). Fig. 10 (c), (e) and (f) show the fracture edges at 300°C. At this temperature, the specimens resulted in two distinct types of failure and fracture edges (i) shear band fracture at 45 degree to the loading axis and (ii) a more gross deformation with cup & cone type ductile rupture. This behaviour was observed in claddings of both the bundles and a similar behaviour has been reported in ref. [9, 10].







Bundle nos.	As fabricated	Bundle-1		Bundle-2		
Temp.(°C)	RT	RT	300	RT	300°C	
						
	(a)	(b)	(c)	(d)	(e)	(f)

Fig. 10 Deformation behaviour of tested specimens

5. Summary:

Post Irradiation Examination of PHWR fuel bundles irradiated to a burnup of 10000 MWd/tU and 22000 MWd/tU was carried out to assess the performance of the fuel pins. The results obtained from the examination is summarised below:

- All the fuel pins of the two fuel bundles were intact with all its appendages in place. Circumferential parallel lines were observed on all the outer fuel pins of bundle-2 which were confirmed to be ridges with ridge height in the range of 30-50 μm .
- Energy spectrum obtained by gamma scanning showed uniform burnup distribution and the distinct peaks of Cs^{137} and Cs^{134} in both the bundles.
- Fission gas analysis of the released gases showed a higher % release in the outer fuel pins as compared to intermediate and central fuel pins of bundle-2. Negligible gas release was observed in the fuel pins of bundle-1.
- Microstructural examinations showed intergranular porosity region and grain growth region in the central portion of the cross section of the outer fuel pin of bundle-2.
- Transverse tensile properties of the cladding estimated from RTT showed a TE of around 6-10% and 5-7% for bundle-1 & bundle-2, respectively at 25°C. Whereas, the TE increased up to 24% for bundle-1 and 22% for bundle-2 at 300°C.

6. References:

- [1]. D. N. Sah, U. K. Viswanathan, E. Ramadasan, K. Unnikrishnan, S. Anantharaman, Journal of Nuclear Materials, 383 (2008) 45-53.
- [2]. Prerna Mishra, D. N. Sah, Sunil Kumar, S. Anantharaman, Journal of Nuclear Materials, 429 (2012) 257-262.
- [3]. D. N. Sah, U. K. Viswanathan, S. Anantharaman, Transactions of the Indian Institute of Metals, C-85, Vol. 63, Issues 1-2, February-April 2010.
- [4]. D. N. Sah, U. K. Viswanathan, K. Unnikrishnan, Prerna Mishra, R. S. Shrivastaw, S. Anantharaman, Post irradiation examination of high burnup PHWR fuel bundle 56504 from KAPS-1, BARC/2007/E/002, BARC, Mumbai, India.
- [5]. Rakesh Soni, P. N. Prasad, S. Vijayakumar, A. G. Chhatre, K. P. Dwivedi (2005) Fuel technology evolution for Indian PHWRs. Nuclear Power Corporation of India Ltd. (NPCIL), India
- [6]. S. S. Bajaj, A. R. Gore, Nuclear Engg. & Design 236 (2006) 701-722.
- [7]. M. V. Parikh, K. Muthu Kumar and R. Padhy, Experience of irradiating PHWR fuel bundles up to a burn-up of 20000 MWd/tU at KAPS, C6, INSAC-2003, Kalpakkam, Chennai, India.
- [8]. S. Chatterjee, S. Anantharaman, K. S. Balakrishnan and K. S. Sivaramakrishnan, Report BARC/I-63, 1981, BARC, Mumbai.
- [9]. A. M. Garde, Zirconium in the Nuc. Ind., Eighth Int. Symp., ASTM STP 1023, pp. 548-569.
- [10]. J. S. Dubey, Sunil Kumar, P. Mishra, V. D. Alur, P. K. Shah, S. Anantharaman, 4-6 January 2010, 20th annual conference of INS (INSAC-2009), Chennai, India.